

1900-Pos**Cortical Oscillations as a Model for Studying Cytoskeleton Regulation During Cell Spreading**

Nancy Costigliola, Maryna Kapustina, Gabriel Weinreb, Timothy Elston, Ken Jacobson.
UNC Chapel Hill, Chapel Hill, NC, USA.

Cell spreading and attachment are integral to multiple physiological processes including wound healing, immune cell-antigen recognition, and tumor cell metastasis. We have discovered that Swiss 3T3 fibroblasts and CHO cells undergo periodic oscillations of the cell body during cell spreading that last from .5 hours after attachment to 1.5 hours and longer. The amplitude and duration of the oscillating phenotype are increased when microtubules are depolymerized. Previously we developed a mechanochemical ODE model describing a possible negative feedback from actomyosin based contractility to stretch-activated calcium channels in propagating cell oscillations. Cortical oscillations provide an ideal model for studying cytoskeleton regulation because the oscillation mechanism is easily quantifiable through the relative phase, amplitude, and period of native oscillations vs. those that have experienced perturbations. Further, we examine the spatiotemporal distribution of $[Ca^{2+}]$ during cell oscillations. We propose that the interplay of the calcium and Rho A pathways both contribute to the propagation of cortical oscillations, with high levels of active Rho A replacing the need for highly dynamic calcium signaling.

1901-Pos**Foraging Strategies for Starving and Feeding Amoeba**

Simon F. Norrelykke, Edward C. Cox.
Princeton University, Princeton, NJ, USA.

Do individual cells have a search strategy when their target is outside their range of detection? Does this strategy change when a high density of targets is encountered?

To answer these questions, we observed single, well-isolated cells of the social amoeba *Dictyostelium* as they forage for bacteria on a flat surface. Time-lapse movies of this predator-prey system were recorded and analyzed. By varying the concentration of the food source over several orders of magnitude the dynamics of the amoebae as they responded to their environment could be studied.

At low bacterial density the amoebae scooped up the bacteria as they passed over them without any detectable change in motion. At higher bacterial density the amoebae slowed down, picking up essentially all bacteria encountered, and were found to change their long-timescale behavior from an unbiased random walk to a self-avoiding random walk. This way the amoebae avoids searching for food in already depleted regions. A single amoeba typically ingested 250 bacteria before pausing for 15 min to divide.

1902-Pos**Cell Elastic Modulus Cytometry using Diode-Bar Optical Stretchers**

Ihab Sraji¹, Justin Chichester², Erich Hoover², Ralph Jimenez³, Jeff Squier², Charles D. Eggleton¹, David W.M. Marr².

¹University of Maryland Baltimore County, Baltimore, MD, USA, ²Colorado School of Mines, Golden, CO, USA, ³University of Colorado, Boulder, CO, USA.

The mechanical deformation of biological cells using optical forces is an efficient experimental method to study cellular mechanical properties that may identify cell types and detect disease states. However, the low throughput has significantly limited its utility and application due to the need to sequentially isolate and probe individual cells. We have implemented a pseudo steady-state high-throughput optical stretcher in which anisotropic forces from an inexpensive laser diode stretch osmotically swollen bovine erythrocytes in a continuous microfluidic flow at a rate of ~ 1 cell/second. This measurement rate is a factor of 10-100 higher than previous demonstrations of optical stretching. We also simulate the deformation of elastic capsules induced by single diode-bar optical stretcher with and without flow. Finally, we demonstrate how theory can be applied to determine the elastic modulus of individual cells from experimental measurements of the equilibrium deformation. Analysis of the deformed cells results in a shear modulus in the range of reported values from 2.5×10^{-3} dyne/cm to 1.3×10^{-2} dyne/cm for swollen human erythrocytes. This new optical approach has the potential to be readily integrated with other cytometric technologies, and with the capability of measuring cell populations, thus enabling true mechanical-property based cytometry.

1903-Pos**Isoform-Specific Contributions of Alpha-Actinin to Glioma Cell Mechanobiology**

Shamik Sen, Sanjay Kumar.

Univ. of California, Berkeley, Berkeley, CA, USA.

Glioblastoma Multiforme (GBM) is a malignant astrocytic tumor associated with low survival rates because of aggressive infiltration of tumor cells into the brain parenchyma. Expression of the actin binding protein alpha-actinin has been strongly correlated with the invasive phenotype of GBM in vivo. To probe the cellular basis of this correlation, we have suppressed expression of the nonmuscle isoforms alpha-actinin-1 and alpha-actinin-4 and examined the contribution of each isoform to the structure, mechanics, and motility of human glioma tumor cells in culture. While subcellular localization of each isoform is distinct, suppression of either isoform yields a phenotype that includes dramatically reduced motility, compensatory upregulation and redistribution of vinculin, reduced cortical elasticity, and reduced ability to adapt to changes in the elasticity of the extracellular matrix (ECM). Mechanistic studies reveal a reciprocal relationship between alpha-actinin and non-muscle myosin II in which depletion of either alpha-actinin isoform reduces myosin expression and maximal cell-ECM tractional forces, and inhibition of myosin-mediated contractility alters subcellular distribution of both isoforms of alpha-actinin. Our results demonstrate that both alpha-actinin-1 and alpha-actinin-4 make critical and distinct contributions to cytoskeletal organization, rigidity-sensing, and motility of glioma cells, thereby yielding mechanistic insight into the observed correlation between alpha-actinin expression and GBM invasiveness in vivo.

1904-Pos**The Optical Mouse Trap: in Vivo Probing of Capillary Viscoelasticity**

Nadja Nijenhuis¹, Marcel Bremerich², Hans Vink³, Jos A.E. Spaan¹, Christoph Schmidt².

¹Academic Medical Center, University of Amsterdam, Amsterdam, Netherlands, ²Georg-August-Universität Göttingen, Göttingen, Germany,

³Cardiovascular Research Institute, Maastricht University, Maastricht, Netherlands.

Optical traps have proven to be a versatile quantitative non-contact manipulation tool. We here demonstrate an optical trap in vivo. We used it to perform microrheology and measure viscoelasticity inside capillaries of a living mouse. We also studied particle interactions with the vascular endothelial boundary layer. It has been reported that the lumen of capillaries is covered with a very sensitive at least 0.5 μ m thick polymer layer, the endothelial glycocalyx (EG) which is extruded by and attached to the endothelial cells that line the inside of blood vessels. The EG is crucial for the chemical and physical protection of the vessel wall and also serves as a mechanosensor for shear flow. We found no indication of elastic response, suggesting the EG is a primarily viscous polymer layer. We also observed the adhesive interaction of blood platelets with the vessel wall after introducing photo-chemical damage by fluorescence excitation of injected dye.

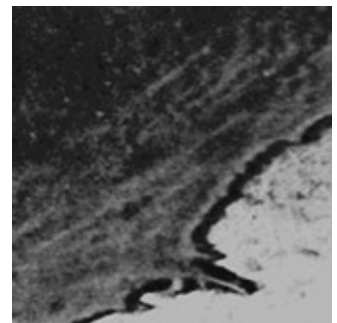
1905-Pos**Mapping Elasticity Down to the Molecular Scale: a Novel High-Resolution Approach to Study Cell Mechanics**

Claudia Friedsam^{1,2}, Donald E. Ingber³, David A. Weitz², Ozgur Sahin¹.

¹Rowland Institute at Harvard, Cambridge, MA, USA, ²Dept. of Physics, Harvard University, Cambridge, MA, USA, ³Wyss Institute for Biologically Inspired Engineering at Harvard University, Children's Hospital, and Harvard Medical School, Boston, MA, USA; Harvard School of Engineering & Applied Sciences, Cambridge, MA, USA, Boston, MA, USA.

The mechanical properties of cells govern a variety of processes critical for the control of their behavior, and they are strongly determined by the cytoskeleton. These observations have inspired numerous studies on cells and reconstituted cytoskeletal networks. However, it remains a challenging task to relate structural and mechanical properties on the molecular scale within living materials.

To analyze cell mechanical properties on the molecular scale, we used recently developed torsional harmonic cantilevers to obtain high-speed force-distance curves in parallel to high-resolution AFM tapping mode images in fluid. By applying this technique, we were able to acquire stiffness maps of



living cells at an unparalleled spatial and temporal resolution (50–100 nm, 4–8 min for a 30 μ m scan). Furthermore, we were also able to map the elasticity of a reconstituted actin network, which has not been achieved before. In combination with optical techniques this opens up a unique simultaneous view of the mechanics of the living cell and the mechanical properties of its relevant molecular components.

Elasticity maps of a live HUVEC cell (30 μ m scan)

1906-Pos

What is Measured By Passive Microbead Rheology?

Jay D. Schieber, Ekaterina Pilyugina.

Illinois Institute of Technology, Chicago, IL, USA.

It is often claimed that the dynamic modulus G^* of a viscoelastic medium can be measured by following the trajectory of a small bead subject to Brownian motion. In the pioneering manuscript that introduced the idea [T. Mason and D. Weitz, *Physical Review Letters* 74, 1250 (1995)], this equivalence between the autocorrelation function and G^* was assumed. Later work claimed that a correspondence could be proven, but to our knowledge, the proof has never been shown. We use here an analytic solution of the forces on a sphere undergoing arbitrary displacement in an arbitrary viscoelastic medium combined with the fluctuation-dissipation theorem to derive what is actually measured in the microbead rheology experiment. We find that a convolution of G^* is indeed measured in the followed autocorrelation function. Under certain restrictions the autocorrelation function is a direct measurement of the dynamic modulus as is typically used. We examine experimental data published in the literature and are unable to find any data where the restrictions do not hold. Nonetheless, the results suggest that the technique could also be used at higher frequencies, if proper analysis is made of the data.

1907-Pos

Intracellular Diffusion in Fission Yeast Cells Depends on Cell Cycle Stage

Christine Selhuber-Unkel¹, Pernille Yde¹, Kirstine Berg-Sørensen², Lene Oddershede¹.

¹Niels Bohr Institute, Copenhagen, Denmark, ²Danish Technical University, Kgs. Lyngby, Denmark.

During the cell cycle, rearrangements of the cytoskeletal network play an essential role, in particular for the success of cell division. In order to quantify the influence of cytoskeletal rearrangements on the viscoelastic properties of the intracellular space, we studied the diffusion of endogenous lipid granules within single fission yeast cells in the different stages of the cell cycle. The position of the granules was tracked with optical tweezers at nanometer and sub-millisecond resolution and the data were analyzed with a power spectral analysis. We found that the majority of the lipid granules underwent subdiffusive motion during all stages of the cell cycle, i.e. the mean squared displacement of the granule is $2Dt^\alpha$ with $\alpha < 1$. With our experiments we have shown that α is significantly smaller during interphase than during any stage of mitotic cell division and, surprisingly, we did not find significant differences of α in the different stages of cell division. These results indicate that the cytoplasm is more elastic during interphase than during cell division and that its elasticity is relatively constant during the stages of cell division.

1908-Pos

A Comparison of Single-Cell Elasticity of Osteogenic Cells Measured with the Optical Stretcher and Holographic Microscope

Michael G. Nichols, Anya K. Burkart, Joy L. Chaput, Robert P. Thomen, Kristina G. Ward, Semere M. Woldemariam.

Creighton University, Omaha, NE, USA.

While it has been known for some time that bone mass is remodeled in response to mechanical stress, the identity of the primary mechanosensor has yet to be clearly established. To determine if cellular elasticity may play a role in the cell's ability to detect a pressure variation, we have used the optical stretcher to measure the elasticity of individual osteogenic cells. To determine cell elasticity from measurements of cellular deformation, the optical pressure on the cell surface is computed using a ray optics model which assumes a value for the index of refraction of the cell. Previously we have estimated this value from measurements of other eukaryotic cells, but the optical pressure varies significantly with small changes in refractive index. Therefore, digital holographic microscopy is used to improve estimates of this critical parameter. We consider the overall impact that a spatial variation in the index of refraction can have on the determination of the optical stress, and compare single-cell elasticity measurements of red blood cells, 2T3 osteoblast and MLO-Y4 osteocyte cells.

* This work was supported by P20 RR016475 from the INBRE Program of the National Center for Research Resources.

Microtubule Motors-Kinesin-1

1909-Pos

An Atomic-Level Engine that Accounts for Kinesin Motility and Catalysis

Charles V. Sindelar¹, Kenneth H. Downing².

¹Brandeis University, Waltham, MA, USA, ²Lawrence Berkeley National

Laboratory, Berkeley, CA, USA.

Kinesin motor proteins convert the energy of ATP hydrolysis into stepping movement along microtubules. In this process, the microtubule can be considered as kinesin's regulatory partner, responsible for activating the enzyme's functional behavior. In the absence of atomic resolution structures describing the kinesin-microtubule complex, the mechanism of this activation has remained unknown. We use cryo-electron microscopy to derive atomic models describing the complete, microtubule-attached, kinetic cycle of a kinesin motor. The resolution of our reconstructions (~8 Å) enabled us to unambiguously build crystallographically-determined conformations of kinesin's key subcomponents into the density maps. The resulting models reveal novel arrangements of kinesin's nucleotide-sensing switch loops and of its microtubule binding element known as the switch II helix. Based on these models, we present a detailed molecular mechanism accounting for kinesin's force generation cycle. In this mechanism, the switch loops control a seesaw-like movement of the catalytic domain relative to the switch II helix, which remains fixed on the microtubule surface. Microtubules couple the seesaw movement to ATP binding by stabilizing the formation of extra coils at the N terminus of the switch II helix, which interact directly with the switch loops. Tilting of the seesaw to assume the ATP-bound orientation in turn elicits a power stroke by the motor domain's force-delivering element known as the neck linker. This sequence of events accounts for the essential mechanics of kinesin's force-delivery cycle, and also yields a new model for the catalytically active conformation of kinesin's ancestral relative, myosin.

1910-Pos

Free Energy Changes During Kinesin's Force-Generating Substep

Wonmuk Hwang¹, Matthew J. Lang², Martin Karplus³.

¹Texas A&M University, College Station, TX, USA, ²MIT, Cambridge, MA, USA, ³Harvard University, Cambridge, MA, USA.

We have previously suggested that Kinesin-1 generates force by transient folding between the N-terminal cover strand and the C-terminal neck linker domains into a beta-sheet, the so-called cover-neck bundle (CNB). Once formed, the CNB has a conformational bias sufficient to move the neck linker forward. Replica exchange molecular dynamics simulations have been performed to elucidate the energetics of CNB formation with and without load. Without load, the CNB state is weakly favorable compared to non-CNB states by 0.85 kcal/mol at 300 K, which is in agreement with a previous experimental value based on electron paramagnetic resonance, 0.72 kcal/mol (Rice et al., *Biophys. J.* 84:1844 (2003)), although the identity of the states involved is not certain. In non-CNB states the mobile neck linker points mostly forward in the ATP-like conformation of the motor head, so there is relatively little conformational difference with the CNB-state. By contrast, when a 10-pN rearward load is applied at the end of the beta9 part of the neck linker, a new local energy minimum appears for a rearward-pointing state. Compared to the CNB state, the free energy of the rearward-pointing state is higher by 2.96 kcal/mol at 300 K. This indicates that the CNB readily forms under applied load and thus is able to move the neck linker forward. The significance of these results for the mechanism by which kinesin-1 walks on microtubules will be discussed.

1911-Pos

Neck-Linker Length is a Critical Determinant of Kinesin Processivity

Shankar Shastry, William Hancock.

Pennsylvania State University, University Park, PA, USA.

The kinesin neck-linker domain is a key mechanical element underlying processive kinesin motility. Not only is neck-linker docking thought to be the dominant conformational change in the kinesin hydrolysis cycle, chemomechanical communication between the two head domains must necessarily be transmitted through the two neck-linker domains and their shared coil-coil. Hence, the length of the neck-linker is expected to have a strong influence on kinesin run length, a quantitative measure of processivity. Across different kinesin families, motors with longer neck-linker domains, such as Kinesin-2 are generally less processive than Kinesin-1, which has the shortest neck-linker domain among N-terminal kinesins. However, there is disagreement in the literature as to whether artificially extending the Kinesin-1 neck-linker alters the motor run length. Using single molecule TIRF analysis to visualize GFP-tagged motors in 80 mM PIPES buffer, we find that lengthening the Kinesin-1 neck-linker by three amino acids results in a five-fold reduction in run length. Consistent